THE JOURNAL OF PHYSICAL CHEMISTRY B

Article

pubs.acs.org/JPCB

Rotational Relaxation in *ortho*-Terphenyl: Using Atomistic Simulations to Bridge Theory and Experiment

Michael P. Eastwood,*[,†] Tarun Chitra,[†] John M. Jumper,[†] Kim Palmo,[†] Albert C. Pan,[†] and David E. Shaw*[,†,‡]

[†]D. E. Shaw Research, New York, New York 10036, United States

[‡]Center for Computational Biology and Bioinformatics, Columbia University, New York, New York 10032, United States

Supporting Information

ABSTRACT: Understanding the nature of the glass transition—the dramatic slowing of dynamics and eventual emergence of a disordered solid from a cooling liquid—is a fundamental challenge in physical science. A central characteristic of glass-forming liquids is a non-exponential main relaxation process. The extent of deviation from exponential relaxation typically becomes more pronounced on cooling. Theories that predict a growth of spatially heterogeneous dynamics as temperature is lowered can explain these observations. In apparent contradiction to these theories, however, some experiments suggest that certain substances—notably including the intensely studied molecular glass-former *ortho*-terphenyl (OTP)—have a main relaxation process whose shape is essentially temperature independent, even though other observables predicted to be correlated with the degree of dynamical heterogeneity are temperature dependent. Here we report the first simulations based on an atomistic model of OTP that reach equilibrium at temperatures well into the supercooled regime. We first show that the results of these simulations are in reasonable quantitative agreement with experimental data for several basic properties over a wide range of temperatures. We then focus on rotational relaxation, finding nearly exponential behavior at high temperatures with clearly increasing deviations as temperature is lowered. The much weaker temperature dependence observed in light-scattering experiments also emerges from the same simulation data when we calculate correlation functions similar to those probed experimentally; this highlights the diversity of temperature dependencies that can be obtained with different probes. Further analysis suggests that the temperature insensitivity observed in the light-scattering experiments stems from the dependence of these measurements on internal as well as rotational molecular motion. Within the temperature range of our OTP simulations, our results strongly suggest that this archetypal glass-former behaves as anticipated by theories of the glass transition that predict increasing non-exponentiality with cooling, and our simulations thus strengthen the evidence supporting such theories.

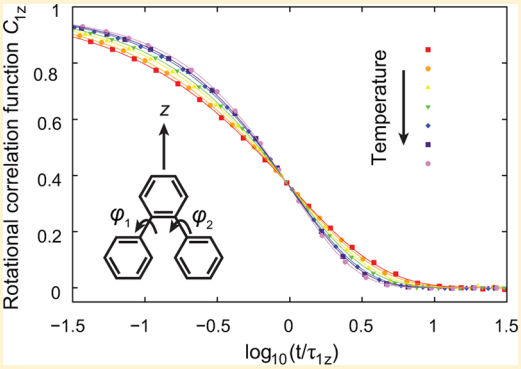

INTRODUCTION

If it avoids crystallization, a liquid will rapidly increase in viscosity when cooled below its melting point, despite apparently modest structural changes. At sufficiently low temperatures, the supercooled liquid can no longer fully relax on experimental time scales—it has become a glass. Development of a firm understanding of the glass transition is often viewed as a grand scientific challenge, and continues to be the subject of much research.[1−3]

One important characteristic of glass-forming liquids, which any viable theory of the glass transition must explain, is the deviation of the main relaxation process from the exponential form typically observed in normal liquids. The main relaxation process is usually reasonably well fit by a stretched exponential form, $A\exp(-(t/\tau)^{\beta})$, with a stretching parameter of $\beta < 1$. The main relaxation in molecular glass-formers typically broadens (becomes more stretched) as the temperature decreases.[4] The degree of stretching at the glass transition is usually greater (β is smaller) for more fragile substances[5] (i.e., those with a markedly non-Arrhenius temperature dependence of relaxation times[6]).

Not all experimental observations fit the pattern of β decreasing with temperature.[7,8] Of particular interest, given its status as an archetypal fragile molecular glass-former, *ortho*-terphenyl (OTP) has recently been found to have a main relaxation process whose shape appears to be temperature independent over a wide temperature range above its glass-transition temperature ($T_g \approx 243$ K).[9,10] These results, which were obtained with dielectric-loss experiments[9] and a combination of light-scattering techniques (photon-correlation spectroscopy (PCS) and experiments using a Fabry−Perot interferometer (FPI)),[10] are similar to earlier results from PCS experiments, which found

Special Issue: Peter G. Wolynes Festschrift

Received: February 28, 2013
Revised: June 3, 2013
Published: July 10, 2013

only modest variation of β with temperature.[11,12] Earlier specific heat-spectroscopy[13] and nuclear magnetic resonance (NMR) measurements,[14] however, found β to vary substantially with temperature.

Here we use long-time-scale simulations of an atomistic model of OTP to probe the temperature dependence of its main relaxation across a wide temperature range (272.5−600 K). Our principal motivation in the work reported here is to determine whether or not OTP has a main relaxation whose shape is independent of temperature, because theories of the glass transition in general often make predictions about the behavior of β. In particular, a constant β would apparently contradict some widely accepted theoretical ideas. As has been emphasized elsewhere,[9] for example, explanations[15−18] of the decoupling between translational and rotational diffusion observed in a number of supercooled liquids (including OTP[19]) in terms of spatially heterogeneous dynamics[20−22] strongly suggest a broadening of relaxation times as the temperature decreases. At a deeper level, random first-order transition (RFOT) theory[23]—a prominent theory of the glass transition, which provides an underlying explanation of the origin of dynamic heterogeneity—makes a firm prediction[24] that β should decrease as a supercooled liquid approaches the glass transition.

OTP has been intensely studied experimentally, and has inspired a simple three-site model[25] widely used in simulations. To provide convincing answers about the anomalous behavior of OTP seen in experiments, however, more realistic models[26−31] in which most or all atoms are represented are likely needed. Computational expense has prevented simulations of such models from adequately sampling the supercooled liquid's slow relaxations at or below the crossover temperature ($T_c \approx 290$ K). This temperature is approximately where decoupling between translational and rotational diffusion sets in,[19] and is thus where β might be anticipated to have a pronounced temperature dependence. At this temperature, however, relaxation times are already on the order of 0.1 μs[32] and rise steeply at lower temperatures. Here, we use Anton, a special-purpose machine for molecular dynamics,[33] to perform fully atomistic simulations of 800 molecules of OTP for up to a few milliseconds.

Our atomistic model came from an in-house biomolecular force field development project, and the parameters were not optimized for OTP in particular. Because of this, and because the intermolecular interactions do not include any special handling of the π-electron distribution, in the first part of the Results section, we assess the accuracy of our model by comparing several properties of OTP in simulation to experimental results. In the body of the paper, we focus primarily on basic dynamic properties, including a quantitative comparison of the decoupling between translational and rotational diffusion seen in experiments and simulations. In an Appendix, we also make comparisons for some basic thermodynamic and structural properties. Together, these comparisons give us confidence that our model provides a quantitatively satisfactory description of OTP over a wide temperature range.

In the second part of the Results section, we focus on the shape of the rotational relaxation of OTP as a function of temperature. We first obtain this shape directly from the correlation function of a vector fixed in the molecular frame, and we find that it is clearly temperature dependent. Using the same simulation data, we then calculate correlation functions that are more closely related to those probed experimentally. This improves the agreement between the simulated and experimental estimates of β, and in the case of the light-scattering experiments provides insight into the slow variation of β with temperature observed in those experiments. Although our simulations cannot fully explain the observations made from the dielectric-loss experiments, our results overall strongly suggest that OTP behaves as many glass-transition theories predict a fragile liquid should, and our simulations further support theoretical ideas consistent with an increased broadening of relaxations with decreasing temperature.

METHODS

Model. All carbon and hydrogen atoms are explicitly represented in our model. Intermolecular interactions are modeled as pairwise-additive interatomic interactions with dispersive, exchange-repulsion, and electrostatic components. The electrostatic component is modeled as a Coulomb interaction between partial point charges of +0.1244 electrons on hydrogen atoms and −0.1244 electrons on carbons that are bonded to hydrogen (the four carbon atoms that are only covalently bonded to other carbon atoms have no partial charge); a switching function is used so that the Coulomb potential is replaced by $(1 - r/r_c)^2/r$ for atom separations r less than a cutoff distance of $r_c = 9$ Å, and for $r \geq 9$ Å, the interactions are zero.[34] The exchange-repulsion interactions are of an exponential form, and the dispersive interactions decay as r^{-6}; both are truncated at 9 Å, and a long-range correction term is added to approximately correct the virial for this truncation. Parameters governing the dispersive and exchange-repulsion interactions are given in the Supporting Information. Apart from rigid constraints of carbon−hydrogen bonds, the molecule is fully flexible; details of the intramolecular interactions are also included in the Supporting Information.

Simulations. There were 800 OTP molecules in the cubic simulation box; periodic boundary conditions were used. OTP was fully deuterated in all simulations, which allows a larger integration time step. Simulations were performed in a temperature range between 272.5 and 600 K; the pressure was 1 bar in all simulations (details of the integration method are in the Supporting Information). We first ran a simulation at 360 K for tens of thousands of rotational relaxation times to generate independent starting configurations. Subsequent simulations were initiated in one of two ways: (i) directly from one of the configurations generated in the 360 K simulation (this method was used at 272.5 K, 277.5 K, ..., 357.5 K, 360 K, 370 K, ..., 600 K, and no two simulations used the same starting structure); (ii) from a configuration taken from the simulation at a 5 K higher temperature after multiple rotational relaxation times have elapsed, resulting in a sequence of simulations at 355 K, 350 K, ..., 275 K. All simulations were longer than 100 rotational relaxation times—the lengths are tabulated in Table S1 (Supporting Information)—and data obtained in the first quarter of all simulations was excluded from further analysis. The configuration of the system was output at regularly spaced time intervals (most commonly a 200 ps interval was used, but at high temperatures, a considerably higher rate was used). To obtain information about dynamics on shorter time scales, configuration data were also output using much shorter time intervals within 100 short trajectory segments that were approximately evenly spaced throughout the last 75% of the trajectory. Simulations of the crystal form were similar to those of the liquid but contained 540 molecules in the simulation cell, were shorter, with more frequent output, and were run using Desmond.[35] The crystal simulations also used anisotropic pressure control, in which the three sides of the orthorhombic

simulation box could vary independently. (Desmond was also used to process the Anton trajectory data to obtain enthalpies.)

Rotational Correlation Functions. We principally examine rotational motion of OTP by examining the relaxation of a unit vector along the *z*-axis. This axis is fixed in the molecular frame, and roughly bisects the bonds from the center ring to the two substituent rings, as shown in Figure 1B (inset). More precisely, we obtain the positive *z*-axis as follows: We take the vector from the molecular center of mass to the center of mass of the carbons of the center ring, and we then project this vector into the best-fit plane through the carbons of the center ring. The *x*-axis is normal to the best-fit plane through the carbons of the center ring (and points away from the viewer if the substituent rings are below the center ring). Finally, $\mathbf{y} = \mathbf{z} \times \mathbf{x}$. The correlation functions for rotation of the *z*-axis are $C_{nz}(t) = \langle P_n(\mathbf{z}(t)\cdot\mathbf{z}(0))\rangle$, where the average is over all molecules and all initial times, and P_n denotes the *n*th order Legendre polynomial ($P_1(x) = x$ and $P_2(x) = (3x^2 - 1)/2$).

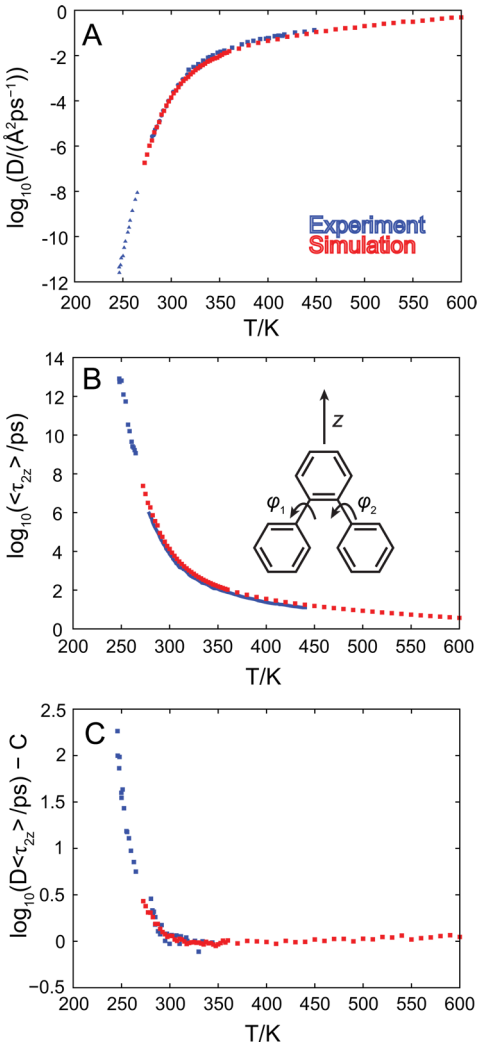

Figure 1. Basic dynamic properties of OTP. Simulation results (red) are compared to experimental results (blue) as a function of temperature for (A) the translational diffusion constant, (B) the average rotational relaxation time, and (C) the product of these two quantities. In part C, both curves are vertically shifted by a constant, *C*, so that they approach zero as the temperature increases. The experimental diffusion constants are from refs 37, 14, and 19 in high-, intermediate-, and low-temperature regimes, respectively; the experimental rotational relaxation times at low temperatures are from ref 14 and at higher temperatures from ref 38. The experimental data for the product shown in part C was taken from ref 19. The inset to part B shows the molecular structure of OTP, the *z*-axis, and the key internal degrees of freedom (φ_1, φ_2). (An angle of zero corresponds to the substituent and center ring being in the same plane; the minimum-energy conformation is close to (φ_1, φ_2) = (50°, 50°), or the mirror image structure at (130°, 130°).)

Molecular Polarizability. The polarizability of a benzene molecule is larger, by almost a factor of 2, in the plane of the ring compared to normal to the ring (see, for example, ref 36). Anticipating that, on the level of the constituent rings, such an effect may be a major source of polarizability anisotropy in OTP, and recognizing that the two substituent rings may rotate relative to the center ring (see inset to Figure 1B), we construct the following model: We assume that the polarizability of an OTP molecule in the lab frame (*X*, *Y*, *Z*) may be approximated as the sum of the polarizabilities of its three constituent rings:

$$\boldsymbol{\alpha} = \sum_{j=1}^{3} \boldsymbol{\alpha}_j = \sum_{j=1}^{3} \mathbf{U}_j \boldsymbol{\alpha}' \mathbf{U}_j^T \tag{1}$$

where *j* runs over the three rings and $U_j = (\nu_{j1}, \nu_{j2}, \nu_{j3})$ is the rotation matrix connecting the body frame of ring *j* and the lab frame; the vectors $\{\nu_{j1}, \nu_{j2}, \nu_{j3}\}$ are orthonormal, with ν_{j3} normal to the best-fit plane through ring *j*. We approximate the polarizability of a ring in its body frame by

$$\boldsymbol{\alpha}' = \begin{pmatrix} \alpha_{\parallel} & 0 & 0 \\ 0 & \alpha_{\parallel} & 0 \\ 0 & 0 & \alpha_{\perp} \end{pmatrix} \tag{2}$$

with the polarizability in the ring plane larger than that in the direction normal to the ring plane, $\alpha_{\parallel} > \alpha_{\perp}$. With our simple model, the molecular polarizability tensor depends on the coordinates only through the normal vectors to the rings:

$$\boldsymbol{\alpha} = 3\alpha_{\parallel}\left(\mathbf{I} - \frac{k}{3}\sum_{j=1}^{3} \boldsymbol{\nu}_{j3}\boldsymbol{\nu}_{j3}^T\right) \tag{3}$$

where **I** is the identity matrix and $k = (\alpha_{\parallel} - \alpha_{\perp})/\alpha_{\parallel}$. We are interested in the autocorrelation functions of the off-diagonal elements of $\boldsymbol{\alpha}$, such as

$$C_{\alpha_{XY}}(t) = \frac{\langle \alpha_{XY}(t + t_0)\alpha_{XY}(t_0)\rangle}{\langle \alpha_{XY}{}^2\rangle} \tag{4}$$

The true equilibrium averages $C_{\alpha_{XY}}(t)$, $C_{\alpha_{YZ}}(t)$, and $C_{\alpha_{ZX}}(t)$ must be equal by symmetry. We estimate the three correlation functions separately and then average them to produce a single estimate we denote C_{α}.

Parameter Fitting. Except where indicated otherwise, stretching exponents were obtained by performing three-parameter least-squares fits of stretched-exponential (also known as Kohlrausch–Williams–Watts, or KWW) functions to correlation functions in the time domain, with the data sampled at times approximately evenly spaced on a logarithmic scale; data from time scales shorter than a 1 ps cutoff were excluded. We denote the time scale parameter using τ (the parameter from fitting C_{2z} is denoted τ_{2z}, for example). We denote average relaxation times using angle brackets ($\langle\tau_{2z}\rangle$, for example), and obtain these using $\langle\tau\rangle = \tau\beta^{-1}\Gamma(\beta^{-1})$.

dx.doi.org/10.1021/jp402102w | J. Phys. Chem. B 2013, 117, 12898–12907

RESULTS

Model Validation. To evaluate the extent to which the simulation model can describe OTP, we have compared a selection of dynamic, thermodynamic, and structural properties to experimental measurements. In this section, we describe results for the translational diffusion constant and rotational relaxation times (Figure 1); the comparisons for thermodynamic and structural properties are described in the Appendix. We calculated the translational diffusion constant, D, from the mean square displacement of the center of mass of OTP molecules as a function of time (note that, in our simulations, OTP is fully deuterated). Figure 1A shows the translational diffusion constant, D, from our simulations compared to three sets of experimental measurements in different temperature ranges. Early NMR measurements[37] gave D in the window 318−448 K, while later work[14] enabled measurements down to 280 K. The simulation results span these temperature ranges and are in good agreement with both sets of data; agreement seems slightly better with the latter experiments, to the extent that the experimental data in Figure 1A is largely obscured by the simulation points. Diffusion in the simulations is slightly lower than that measured experimentally, but the diffusion constant is still ∼70% or more of the experimental value. At lower temperatures, the simulation results also appear to approach the results of measurements made near T_g by isothermally desorbing thin bilayer films of deuterated and nondeuterated OTP.[19] The average rotational relaxation times from simulations similarly appear to be in good agreement with those measured experimentally (Figure 1B), being only 50% slower than those of NMR measurements made in a temperature regime above 280 K,[38] and appearing to approach others made nearer to T_g.[14] Importantly, the product of the translational diffusion constant and the average rotational relaxation time (Figure 1C) shows that decoupling observed in simulations is quantitatively very similar to that seen experimentally.

Taken together with the data presented in the Appendix, these results show that the simulations are in fairly good agreement with experiment for a wide range of properties and temperatures, suggesting that they give a reasonable description of molecular motion in OTP, and thus may give reasonable estimates of quantities that are currently difficult to access experimentally. We now turn to the question of the non-exponentiality of relaxations in OTP, for which the experimental data does not paint a clear picture.

Non-exponential Relaxation. In Figure 2A, we show the KWW stretching exponent obtained in various experiments. (Different experiments using the same basic technique are shown in the same color.) At first glance, the aggregate experimental results appear to emphatically point to a substantial decrease in β as temperature is lowered below ∼300 K. On closer inspection, however, things are much less clear: There are only three experiments that, taken individually, show a steep decrease in β as temperature decreases. One of these, a set of specific heat-spectroscopy measurements[13] (purple in Figure 2A), was performed using OTP with 9% *o*-phenylphenol impurities to suppress crystallization. A second, using depolarized light-scattering[11] (dark blue triangles), used a fitting procedure which has been questioned,[39] and more recent light-scattering studies[10,39] have found an approximately constant β above the crossover temperature (other dark blue points). The third data set, with a strongly temperature-dependent β, is from an NMR study[14] (green triangles), which yields a much lower value of β near T_g than do other methods. Data from PCS[10−12] and dielectric-loss measurements[9,40] suggest either a modest[11,12,40] or no[9,10] temperature dependence for β. Additionally, recent FPI results do not approach $\beta = 1$ at high temperatures,

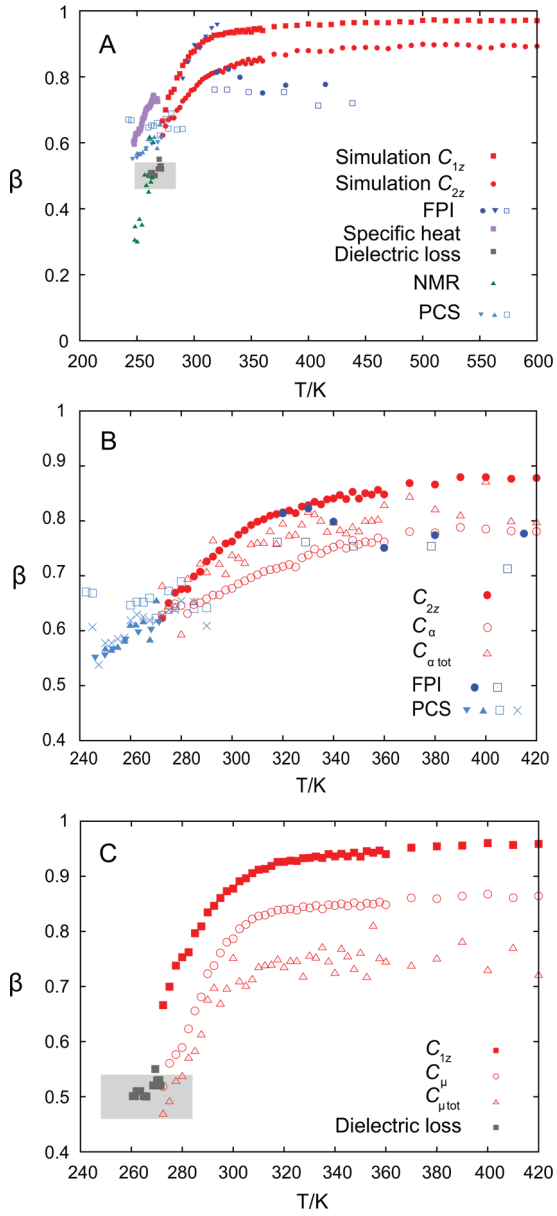

Figure 2. Comparison of KWW stretching exponents obtained in simulation (red) and experiment (other colors). (A) Simulation stretching exponents derived from the C_{1z} and C_{2z} rotational correlation functions, and stretching exponents from a wide variety of experiments that include FPI[39,11,10] (dark blue circles, triangles, and open squares, respectively), specific heat-spectroscopy,[13] dielectric-loss spectroscopy[9,40] (gray shaded region and gray circles, respectively), NMR,[14] and PCS[11,12,10] (light blue down-pointing triangles, up-pointing triangles, and open squares, respectively). (B) Simulation stretching exponents (red) from the (C_{2z}) rotational correlation function, the molecular-polarizability correlation function, and the total-polarizability correlation function. These are compared to data from light-scattering and PCS experiments (same symbols as in part A); the crosses show the results of fitting the data from ref 10 directly to a stretched exponential form. (C) Simulation stretching exponents (red) from the (C_{1z}) rotational correlation function, the dipole correlation function, and the total-dipole correlation function. These are compared to data from dielectric-loss spectroscopy (same symbols as in part A).

dx.doi.org/10.1021/jp402102w | J. Phys. Chem. B 2013, 117, 12898−12907

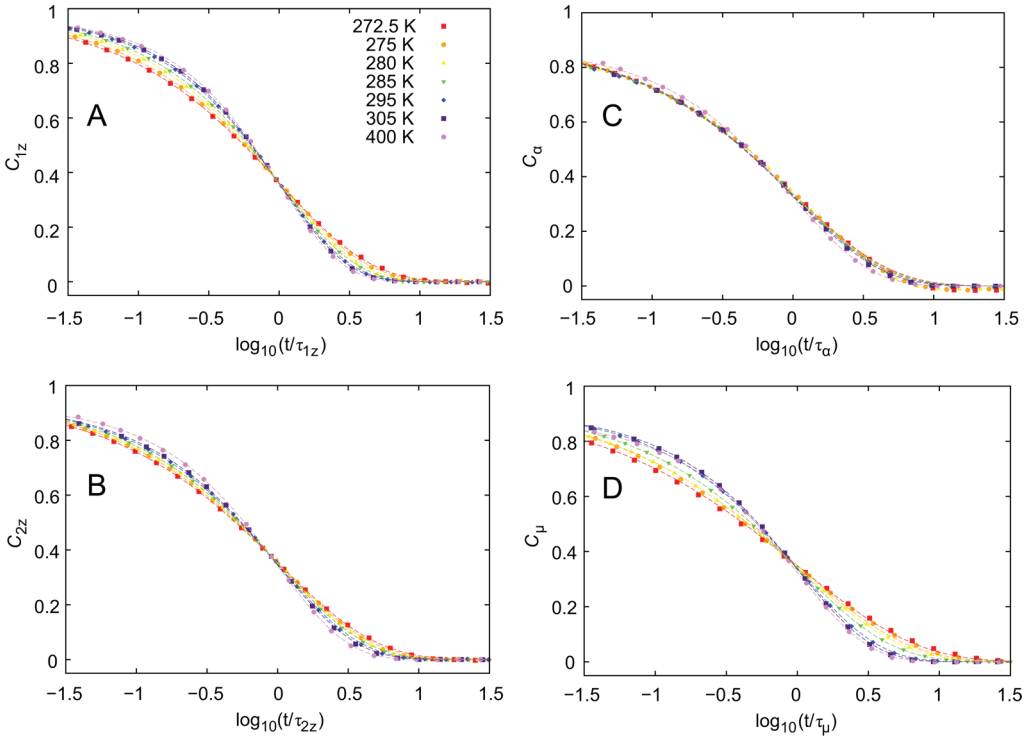

Figure 3. Simulation correlation functions at various temperatures (points) and KWW fits (curves). The functions are plotted as a function of $\log(t/\tau)$, where τ is the time scale obtained in the fit, so that the extent of broadening as the temperature decreases is apparent. The correlation functions shown are (A) the C_{1z} rotational correlation function, (B) the C_{2z} rotational correlation function, (C) the molecular-polarizability correlation function, and (D) the dipole-moment correlation function.

reaching a value of $\beta < 0.8$,[10,39] only modestly higher than the related PCS measurements at lower temperatures; this has led to the suggestion[10] that, as measured by light-scattering, OTP obeys time−temperature superposition (i.e., constant β) from the glass-transition temperature to above the melting point. (We note that transient-grating experiments that probed density fluctuations in OTP also found β to be approximately constant, with a value between 0.5 and 0.6 (with large uncertainties) in the temperature range 270−300 K,[42] and that single-molecule probe experiments showed no trend in the widths of probe relaxation times with variation in temperature in a narrow temperature range close to T_g.[43])

The simulation results for the stretching exponent of the rotational correlation functions C_{1z} and C_{2z} are shown in red in Figure 2A. These were obtained by fitting stretched-exponential functions to the correlation functions, as described in the Methods section. At high temperatures, we find β to be close to 1 and approximately constant; although some decrease in β with decreasing temperature appears to be observable above 300 K, below this temperature there is a prominent drop in β. This behavior is robust to the choice of the axis of rotation and to variation in the fitting procedure, although the precise value β approaches at high temperature depends somewhat on details of the fit (Figure S1, Supporting Information). In addition, direct inspection of the correlation functions as a function of $\log(t)$ shows that they cannot be superimposed by shifting them by $\log(\tau)$; instead, the increased broadening at lower temperatures is clearly evident (Figure 3A,B).

The simulations clearly point to a rapid decrease in β as temperature is lowered through the crossover temperature. Simulation is one of the few techniques that broadly spans this temperature regime, but at either end of the temperature range of the simulations, there is overlap with the temperature range for which various experimental results exist, and notable discrepancies between the simulation and experimental results can be seen. In particular, the simulation results predict a more rapidly varying β than seen in either the dielectric spectroscopy or PCS measurements, and they also predict a higher value of β than seen either in dielectric-loss spectroscopy or FPI measurements.

We now investigate the extent to which these disagreements may come from differences in the correlation functions probed in experiment and simulation. The light-scattering experiments probe polarizability fluctuations of the system. These can arise from density fluctuations and, importantly, from fluctuations in the polarizability tensor in the lab frame as non-isotropic molecules rotate. In the simple case in which molecules (and their translational and rotational motions) are independent, the contribution of molecular rotation to the intensity measured in a depolarized light-scattering experiment with heterodyne detection is proportional to $C_{\alpha\prime}$ the autocorrelation function of the off-diagonal elements of the molecular-polarizability tensor.[44] With the further simplification of cylindrically symmetric molecules about the z-axis, this contribution further reduces to the rotational correlation function C_{2z}.[44] Depolarized light-scattering experiments on supercooled liquids are thus sometimes considered to be approximately probing C_{2z}. In addition to calculating $C_{2z\prime}$ we also estimated C_α by making a simple model for the molecular polarizability, in which we assume that the polarizability of OTP in the lab frame is the sum of that of three independent benzene rings placed at those positions (see Methods). This model takes account of the two key internal degrees of freedom in OTP—the dihedral angles of the two substituent rings relative to the center ring (φ_1, φ_2) shown in Figure 1B. To evaluate the effect of intermolecular correlations, we have also

dx.doi.org/10.1021/jp402102w | J. Phys. Chem. B 2013, 117, 12898−12907

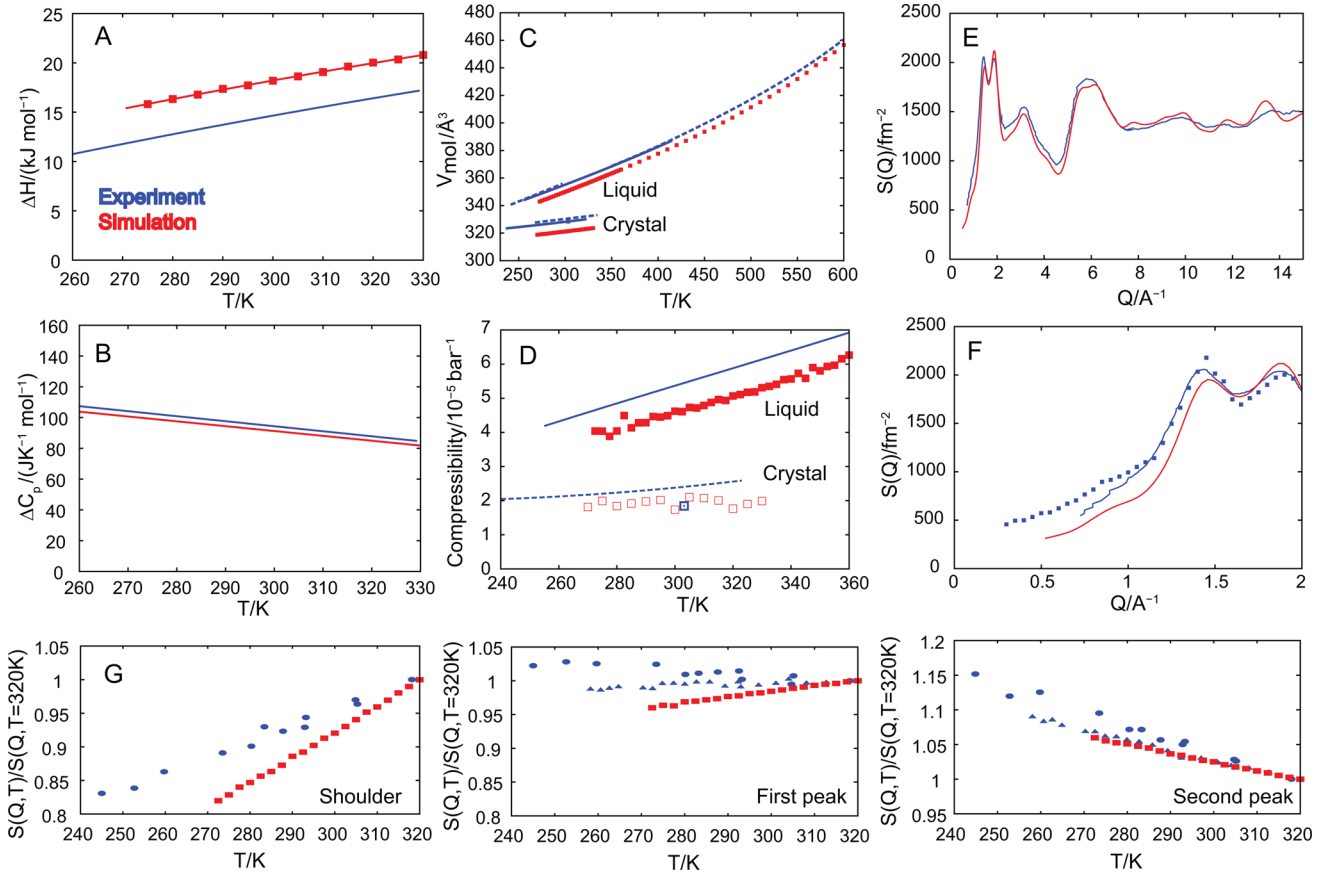

Figure 4. Comparison of thermodynamic and structural properties of OTP in simulation (red) and experiment (blue). (A) Enthalpy difference between liquid and crystal with the red line a best-fit quadratic; (B) heat-capacity difference between liquid and crystal derived from a quadratic fit to enthalpy difference (experimental data from ref 49). (C) Molecular volume as a function of temperature. Experimental data is from three sources. The solid lines are from ref 41, the dashed line for the low-temperature liquid and for the solid are from ref 54, and the dashed line for the high-temperature liquid and the crystal data point at 302 K are from ref 55. (D) Compressibility as a function of temperature; experimental data is shown as lines[41] and a single point.[55] (E) Structure factor obtained in simulation (at 315 K) compared to neutron-scattering results (at 314 K) from ref 52. (F) The structure factor in the low wavevector region; the data shown is the same as in part E, with the additional data (at 320 K) from a more recent experiment[53] (this structure factor was reported in arbitrary units, so it has been multiplied by a constant). (G) Variation in structure factor as a function of temperature at three wavevectors (0.85, 1.45, and 1.95 $Å^{-1}$) corresponding to the approximate locations of the shoulder, first peak, and second peak. Experimental data are circles[53] and triangles[52] (in the latter work, temperature-dependent data were obtained at the slightly different wavevectors 1.4 and 1.9 $Å^{-1}$).

calculated the correlation function $C_{\alpha\,\mathrm{tot}}$, which is the auto-correlation function of the off-diagonal elements of the total polarizability of the simulation box.

In Figure 2B, we show β values from some of the light-scattering experiments (the PCS experiments and the two more-recent FPI experiments). Three simulation curves are also shown in red. The upper curve is from C_{2z} (also shown in Figure 2A) and is in fair agreement with the light-scattering data, but it appears to have a larger slope than the curve of the PCS results in the temperature window in which both simulation and PCS results have been obtained; at high temperatures, the curve levels off to a higher value of β (0.89) than that of the FPI results (between 0.7 and 0.8). The β value obtained from the molecular-polarizability correlation function, C_{α}, appears, by contrast, to agree much better with the light-scattering results. It levels off to a noticeably lower value (~0.75) at high temperatures, and it is notably less dependent on temperature at lower temperatures. Indeed, as illustrated in Figure 3C, it is difficult to perceive by eye any temperature dependence in the shape of the correlation function between 305 and 272.5 K. Including further intermolecular correlations by using the total-polarizability correlation function does not appear to substantially change the results, although this quantity has greater statistical uncertainty. Further investigation (see Figure S4, Supporting Information) shows that the polarizability correlation function of the center ring alone is indeed very similar to C_{2z} but that the correlation functions of the substituent rings differ. The different behavior of C_{α} compared to C_{2z} thus arises from the former's direct dependence on internal motion. Finally, we note that the set of PCS data that suggests a constant β was fit with a Cole–Davidson form.[10] This data (and the FPI measurements from the same source) are shown with open symbols in Figure 2, at positions calculated using an approximate conversion formula (eq 31b from ref 45). Our attempt to directly fit the data of ref 10 to a stretched-exponential function (crosses in Figure 2B), although subject to large uncertainty at the highest and lowest temperatures, suggests that the KWW β obtained from this data may be consistent with the modest temperature dependence found in the other PCS data.

Finally, we compare the simulation results in more detail to the dielectric-loss spectra, which probe fluctuations in the total polarization of the system. The corresponding molecular quantity

dx.doi.org/10.1021/jp402102w | J. Phys. Chem. B 2013, 117, 12898–12907

is the dipole-moment correlation function $C_\mu = \langle \boldsymbol{\mu}(t)\cdot\boldsymbol{\mu}(0)\rangle/\langle\mu^2\rangle$. If a molecule has a permanent dipole moment that is insensitive to intramolecular degrees of freedom, then $C_\mu = C_{1z}$, where z labels the dipole axis. In its minimum-energy configuration, OTP does have a dipole moment pointing along its z-axis, but it is small and thus potentially dependent on the dihedral angles of the substituent rings. We have estimated OTP's dipole moment as a function of these degrees of freedom using quantum calculations (see the Supporting Information). The resulting dipole moment is shown in Figure S3 (Supporting Information) and does exhibit a clear dependence on the dihedral angles.

In Figure 2C, we show the stretching exponents derived from KWW fits to dielectric-loss measurements (the gray points are from ref 40, and the gray rectangle denotes the finding[9] that $\beta = 0.5 \pm 0.04$ in the temperature range 248−284 K). Three simulation curves are also shown: The top one is β obtained from fitting C_{1z} (this data is also shown in Figure 2A), and as noted above, it yields values of β that are noticeably higher than experiment. The molecular-dipole-moment correlation function is, however, substantially shifted to lower β, so that it is only in noticeable disagreement with the experimental data at the very upper end of the experimental temperature range. Including the effects of intermolecular correlations by computing the correlation function of the total dipole moment of the simulation system pushes β down still further. The magnitudes of the values of β from simulation thus appear to be rather similar to those in experiment. The temperature dependence of β observed in the dielectric-loss results is, however, not observed in the simulations. Indeed, as Figure 3D makes apparent, the broadening of the molecular-dipole-moment correlation function is even more marked than that for C_{1z}.

CONCLUSIONS

Overall, our results strongly suggest that OTP behaves in the manner widely anticipated to be canonical for a fragile glass-former, with a clear broadening of rotational relaxations as the temperature is lowered through T_c; the simulations thus add further support to this picture. They also highlight the differences in β values that can be obtained from different probes: Although differences in β values from different experimental techniques are commonly observed, our analysis shows that the temperature dependence observed in different techniques can be large enough that different probes of molecular relaxation can potentially lead to qualitatively different conclusions. Finally, our results show that our model appears to describe OTP with relatively good accuracy, suggesting that more can be learned about the crossover behavior of this archetypal fragile liquid from simulations.

Our simulations span T_c, a region difficult to access experimentally for OTP, but they do not directly address behavior near T_g. Linear extrapolation down to T_g of the β values obtained from the rotational correlation functions C_{1z} and C_{2z} yields values between 0.4 and 0.5, which appear in line with values for similarly fragile liquids (as well as RFOT predictions[24]). Given that the decoupling between rotational and translational diffusion in OTP at the lowest simulation temperature is much less pronounced than it is at T_g, we would expect these β values to continue to decrease outside of the temperature window of the simulations. We cannot, however, determine whether or not this is the case. (A further simulation at the slightly lower temperature of 270 K in fact yielded larger values of β than did the simulation at 272.5 K, but calculation of the energy indicated that this simulation is not fully relaxed and is thus unconverged.)

Although, overall, the agreement of the simulation and experimental results appears to be good, $\beta(T)$ obtained from the total dipole moment appears as if it would ultimately shoot below the results obtained from dielectric-loss experiments to reach much lower values as the temperature is lowered (Figure 2C). It is unclear, however, whether or not our model would predict substantially different values at these temperatures. In the narrow temperature region of overlap between these experiments and simulation results (272.5−284 K), four of five simulation points lie within the experimental error bars, and none lie below them. Additionally, we note that linear extrapolation of the results from the total-dipole correlation function yields $\beta < 0.2$ near T_g, which is an anomalously low value, even for a glass-former of OTP's fragility; this suggests that some leveling off in $\beta(T)$ may well occur before that temperature is reached. It is not obvious what might be responsible for such a leveling off, but it is noteworthy that the substantially higher $\beta(T)$ obtained from C_{1z} compared to that obtained from C_μ shows that intramolecular motion plays a role in the low values obtained from the latter; if the OTP molecule were only allowed to adopt its two gas-phase minimum-energy conformations, these two stretching exponents would be identical. As temperature is lowered, and the OTP molecules remain closer to their low-energy conformations, one would thus expect the gap between the two stretching exponents to narrow. In one (admittedly speculative) scenario, the relatively flat behavior seen in $\beta(T)$ from dielectric-loss experiments might in part reflect a competition between increasingly heterogeneous and cooperative molecular rearrangements that act to decrease β as temperature is lowered, and a waning ability of intramolecular motion to decrease β as the local structure stays closer to its minimum-energy configuration.

A single stretched-exponential form appears to fit our correlation function data reasonably well, but it is not perfect.[4] In the plateau region and the approach to the main decay, our rotational correlation functions decay more rapidly than suggested by a stretched-exponential form, an observation consistent with the existence of processes faster than the main relaxation but slower than the rattling motion of caged molecules. The value of β obtained from a single stretched-exponential fit will to some extent depend on these faster processes, which complicates the interpretation of β.[46] It has further been suggested that a high-frequency excess wing to a main relaxation of temperature-independent width may be able to explain temperature variation of β.[46] Although such high-frequency processes likely contribute to the values of β obtained in our simulations, the changing shape of our rotational correlation functions with temperature in the long-time tail (seen, for example, in Figure 3A) strongly suggests that in OTP the main relaxation process itself broadens as temperature decreases.

In this work, we have used a detailed atomistic model because its good quantitative agreement with experiment greatly strengthens our conclusion that for OTP stretching of rotational relaxation increases with decreasing temperature. Additionally, our detailed model allows us to examine the effect of intramolecular interactions, which our results show play an important role in modulating the different relaxation functions. A sizable part of our current understanding of supercooled liquids and glasses, however, comes from simulations with coarse-grained models, so a natural question is whether a coarse-grained model of OTP, such as the Lewis−Wahnström model,[25] would predict

the same trend in $\beta(T)$ for rotational relaxation as we have observed here. Interestingly, the rotational relaxation functions for this model presented in the work of Lombardo et al.[47] do not appear to show any clear trend in $\beta(T)$; our fit to the functions presented in their Figure 6, which correspond to our C_{2z}, suggests that β lies between 0.8 and 0.9, with a slightly higher value at the lowest temperature. Given that Lombardo et al. find the product $D\langle\tau_{2z}\rangle$ to show a large deviation from its high-temperature value only at the lowest temperature studied, the approximately constant stretching over most of their temperature range is consistent with the atomistic simulation results, but it would be interesting to understand why the Lewis–Wahnström model β is not smaller at the lowest temperature studied (where decoupling is clearly evident). We note that rotational relaxation has been studied in other coarse-grained models not inspired by OTP: Chong and Kob, for example, were able to provide a detailed explanation for decoupling in terms of dynamical heterogeneity using a rigid-rotor model.[48] Their rotational correlation functions show no strong trend in $\beta(T)$, although our fits suggest β may modestly decrease from slightly over 0.9 at the highest temperature studied to just under 0.8 at the lowest temperature for which correlation function data was presented. It would be interesting to know whether a stronger decrease in β is observed at lower temperatures, where the decoupling was substantial.

Our results contribute to the body of evidence supporting theories that predict fragile glass-formers to have increasingly pronounced non-exponentiality as temperature decreases. This prediction is fairly well accepted—particularly in the region near the crossover temperature—thus, although we believe our work provides valuable clarification of the intriguing behavior of OTP, our results are perhaps not entirely surprising. More controversial is the underlying origin of these commonly observed behaviors. In the future, we hope to take advantage of the full description of molecular motion contained in our simulations to help address these deeper questions.

APPENDIX

In this Appendix, we compare several thermodynamic and structural quantities obtained in our simulations with experiment. The results are shown in Figure 4, which is intended to complement the dynamic comparisons in Figure 1. By performing additional simulations starting from the crystal conformation in the temperature range 270–330 K, we have been able to calculate the enthalpy difference, ΔH, between the liquid and crystal phases. This is plotted in Figure 4A, along with the results of experimental calorimetric measurements.[49] We find that the enthalpy difference is only about 3.7 kJ mol^{-1} higher in the simulations. We estimate the simulation heat capacity by first fitting the enthalpy data with a second-order polynomial in temperature (the curve through the simulation points in Figure 4A) and then obtaining a linear estimate of the heat capacity by differentiation. The latter is shown in Figure 4B and is only 3–4% smaller than the experimental value, indicating that the simulations accurately describe the rate of change of configurational entropy with temperature.

The approximately constant difference of 3.7 kJ mol^{-1} between the simulation and experimental enthalpies of melting is probably in part attributable to the model underestimating the contribution of intramolecular strain to the enthalpy of the crystal. The conformation adopted by OTP molecules in the crystal (62°, 42°)[50,51] appears to be somewhat strained, reflecting a frustration between competing intra- and intermolecular interactions. Quantum calculations (see the Supporting Information) suggest that our model correctly identifies the minimum-energy conformation but that it underestimates the energetic cost of deviating from it (Figure S2, Supporting Information). At (60°, 40°), the nearest grid point in our quantum calculations to the crystal conformation, the strain is 5.8 kJ mol^{-1}, compared to 2.2 kJ mol^{-1} in our model. The difference of 3.6 kJ mol^{-1} appears to explain the higher enthalpy of melting observed in the simulations, although it is quite possible that there are similarly sized contributions to the enthalpy-of-melting error that happen to cancel.

Neither the model's somewhat less restricted internal motion nor its other approximations appear to have a substantial impact on the temperature variation of the structure of OTP observed in the simulations. The molecular volumes (Figure 4C) are similar over a wide temperature range, and the simulations give a system that is only about 1.5% denser than experiment (about 2% for the crystal). The thermal expansivity of OTP in simulation is also similar to experiment (for example, at 300 K, the simulation value for the liquid is 7.4×10^{-4} K^{-1}, compared to the experimental value[41] of 7.2×10^{-4} K^{-1}). OTP's compressibility in simulation, which was computed from the volume fluctuations, is not captured quite so accurately (Figure 4D). It is, nevertheless, only about 15% less than the experimental value for both the liquid and the crystal, and its temperature dependence is similar to that seen experimentally. Figure 4E shows the structure factor in simulation compared to that measured by neutron scattering[52] on the same absolute scale (see the Supporting Information). The same data, together with more recent neutron-scattering measurements,[53] appears in Figure 4F for small wavevectors, where most of the temperature variation in the structure factor occurs both in simulation and experiment. This temperature variation is shown in Figure 4G, where the relative change in the structure factor with temperature is plotted for three features in the spectrum: the shoulder (around 0.85 Å^{-1}), the first peak (around 1.45 Å^{-1}), and the second peak (around 1.95 Å^{-1}). The temperature dependence of the three features is similar in simulation and experiment. The propensity of the simulations to underestimate the height of the features as temperature decreases, a tendency noticeable at lower wavenumbers, may be connected to the relative error in the compressibility, which is slightly larger in relative terms at lower temperatures (Figure 4D).

ASSOCIATED CONTENT

Supporting Information

Details of the integration method, further details of the model, details of the structure factor and quantum calculations, a list of simulation lengths and rotational correlation times, and additional figures. This material is available free of charge via the Internet at http://pubs.acs.org.

AUTHOR INFORMATION

Corresponding Author

*E-mail: Michael.Eastwood@DEShawResearch.com (M.P.E.); David.Shaw@DEShawResearch.com (D.E.S.). Phone: (212) 478-0787 (M.P.E.); (212) 478-0260 (D.E.S.). Fax: (212) 845-1787 (M.P.E.); (212) 845-1286 (D.E.S.).

Notes

The authors declare the following competing financial interest(s): This study was conducted and funded internally by D. E. Shaw Research, of which D.E.S. is the sole beneficial

owner and Chief Scientist, and with which all authors are affiliated.

■ ACKNOWLEDGMENTS

We thank Brent Gregersen, John Klepeis, and Je-Luen Li for helpful discussions and contributions to the broader in-house force field development project from which the force field for OTP was obtained. We thank Berkman Frank for editorial assistance.

■ REFERENCES

(1) Ediger, M. D.; Harrowell, P. Perspective: Supercooled Liquids and Glasses. *J. Chem. Phys.* **2012**, *137*, 080901.
(2) Wolynes, P. G.; Lubchenko, V. *Structural Glasses and Supercooled Liquids: Theory, Experiment, and Applications*; John Wiley & Sons: New York, 2012.
(3) Biroli, G.; Garrahan, J. P. Perspective: The Glass Transition. *J. Chem. Phys.* **2013**, *138*, 12A301.
(4) Dixon, P. K.; Wu, L.; Nagel, S. R.; Williams, B. D.; Carini, J. P. Scaling in the Relaxation of Supercooled Liquids. *Phys. Rev. Lett.* **1990**, *65* (9), 1108−1111.
(5) Böhmer, R.; Ngai, K. L.; Angell, C. A.; Plazek, D. J. Nonexponential Relaxations in Strong and Fragile Glass Formers. *J. Chem. Phys.* **1993**, *99* (5), 4201−4209.
(6) Angell, C. A. Relaxation in Liquids, Polymers and Plastic Crystals—Strong/Fragile Patterns and Problems. *J. Non-Cryst. Solids* **1991**, *131*−*133*, 13−31.
(7) Olsen, N. B.; Christensen, T.; Dyre, J. C. Time-Temperature Superposition in Viscous Liquids. *Phys. Rev. Lett.* **2001**, *86* (7), 1271−1274.
(8) Richert, R.; Duvvuri, K.; Lien-Thi, D. Dynamics of Glass-Forming Liquids. VII. Dielectric Relaxation of Supercooled *tris*-Naphthylbenzene, Squalane, and Decahydroisoquinoline. *J. Chem. Phys.* **2003**, *118* (4), 1828−1836.
(9) Richert, R. On the Dielectric Susceptibility Spectra of Supercooled o-Terphenyl. *J. Chem. Phys.* **2005**, *123* (15), 154502.
(10) Petzold, N.; Rössler, E. A. Light Scattering Study on the Glass Former o-Terphenyl. *J. Chem. Phys.* **2010**, *133* (12), 124512.
(11) Steffen, W.; Patkowski, A.; Gläser, H.; Meier, G.; Fischer, E. W. Depolarized-Light-Scattering Study of Orthoterphenyl and Comparison with the Mode-Coupling Model. *Phys. Rev. E* **1994**, *49* (4), 2992−3002.
(12) Hwang, Y.-H.; Shen, G. Q. A Study of α-Relaxation in ortho-Terphenyl by Photon Correlation Spectroscopy. *J. Phys.: Condens. Matter* **1999**, *11* (6), 1453−1462.
(13) Dixon, P. K.; Nagel, S. R. Frequency-Dependent Specific Heat and Thermal Conductivity at the Glass Transition in o-Terphenyl Mixtures. *Phys. Rev. Lett.* **1988**, *61* (3), 341−344.
(14) Fujara, F.; Geil, B.; Sillescu, H.; Fleischer, G. Translational and Rotational Diffusion in Supercooled ortho-Terphenyl Close to the Glass Transition. *Z. Phys. B: Condens. Matter* **1992**, *88* (2), 195−204.
(15) Stillinger, F. H.; Hodgdon, J. A. Translation-Rotation Paradox for Diffusion in Fragile Glass-Forming Liquids. *Phys. Rev. E* **1994**, *50* (3), 2064−2068.
(16) Tarjus, G.; Kivelson, D. Breakdown of the Stokes−Einstein Relation in Supercooled Liquids. *J. Chem. Phys.* **1995**, *103* (8), 3071−3073.
(17) Cicerone, M. T.; Wagner, P. A.; Ediger, M. D. Translational Diffusion on Heterogeneous Lattices: A Model for Dynamics in Glass Forming Materials. *J. Phys. Chem. B* **1997**, *101* (43), 8727−8734.
(18) Xia, X.; Wolynes, P. G. Diffusion and the Mesoscopic Hydrodynamics of Supercooled Liquids. *J. Phys. Chem. B* **2001**, *105*, 6570−6573.
(19) Mapes, M. K.; Swallen, S. F.; Ediger, M. D. Self-Diffusion of Supercooled o-Terphenyl near the Glass Transition Temperature. *J. Phys. Chem. B* **2006**, *110* (1), 507−511.
(20) Ediger, M. D. Spatially Heterogeneous Dynamics in Supercooled Liquids. *Annu. Rev. Phys. Chem.* **2000**, *51*, 99−128.
(21) Glotzer, S. C. Spatially Heterogeneous Dynamics in Liquids: Insights from Simulation. *J. Non-Cryst. Solids* **2000**, *274* (1), 342−355.
(22) Sillescu, H. Heterogeneity at the Glass Transition: A Review. *J. Non-Cryst. Solids* **1999**, *2*−*3*, 81−108.
(23) Lubchenko, V.; Wolynes, P. G. Theory of Structural Glasses and Supercooled Liquids. *Annu. Rev. Phys. Chem.* **2007**, *58*, 235−266.
(24) Xia, X.; Wolynes, P. G. Microscopic Theory of Heterogeneity and Nonexponential Relaxations in Supercooled Liquids. *Phys. Rev. Lett.* **2001**, *86* (24), 5526−5529.
(25) Lewis, L. J.; Wahnström, G. Molecular-Dynamics Study of Supercooled ortho-Terphenyl. *Phys. Rev. E* **1994**, *50* (5), 3865−3877.
(26) Kudchadkar, S. R.; Wiest, J. M. Molecular Dynamics Simulations of the Glass Former ortho-Terphenyl. *J. Chem. Phys.* **1995**, *103* (19), 8566−8576.
(27) Ghosh, J.; Faller, R. A Comparative Molecular Simulation Study of the Glass Former *ortho*-Terphenyl in Bulk and Freestanding Films. *J. Chem. Phys.* **2006**, *125*, 044506.
(28) Mossa, S.; Di Leonardo, R.; Ruocco, G.; Sampoli, M. Molecular Dynamics Simulation of the Fragile Glass-Former Orthoterphenyl: A Flexible Molecule Model. *Phys. Rev. E* **2000**, *62* (1), 612−630.
(29) Mossa, S.; Ruocco, G.; Sampoli, M. Molecular Dynamics Simulation of the Fragile Glass-Former Orthoterphenyl: A Flexible Molecule Model. II. Collective Dynamics. *Phys. Rev. E* **2001**, *64* (1), 021511.
(30) Berry, R. J.; Rigby, D.; Duan, D.; Schwartz, M. Molecular Dynamics Study of Translational and Rotational Diffusion in Liquid ortho-Terphenyl. *J. Phys. Chem. A* **2006**, *110*, 13−19.
(31) Ou, J. J.; Chen, S. H. Molecular Dynamics Simulation of Organic Glass Formers: I. *ortho*-Terphenyl and 1,3,5-Tri-α-naphthyl Benzene. *J. Comput. Chem.* **1998**, *19* (1), 86−93.
(32) Novikov, V. N.; Sokolov, A. P. Universality of the Dynamic Crossover in Glass-Forming Liquids: A "Magic" Relaxation Time. *Phys. Rev. E* **2007**, *67*, 031507.
(33) Shaw, D. E.; Dror, R. O.; Salmon, J. K.; Grossman, J. P.; Mackenzie, K. M.; Bank, J. A.; Young, C.; Deneroff, M. M.; Batson, B.; Bowers, K. J.; et al. Millisecond-Scale Molecular Dynamics Simulations on Anton. *Proceedings of the Conference on High Performance Computing, Networking, Storage, and Analysis (SC09)*; ACM Press: New York, 2009.
(34) Brooks, C. L., III; Pettitt, B. M.; Karplus, M. Structural and Energetic Effects of Truncating Long Ranged Interactions in Ionic and Polar Fluids. *J. Chem. Phys.* **1985**, *83* (11), 5897−5908.
(35) Bowers, K. J.; Chow, E.; Xu, H.; Dror, R. O.; Eastwood, M. P.; Gregersen, B. A.; Klepeis, J. L.; Kolossváry, I.; Moraes, M. A.; Sacerdoti, F.; et al. Novel Algorithms for Scalable Molecular Dynamics Simulations on Commodity Clusters. *Proceedings of the ACM/IEEE Conference on Supercomputing (SC06)*; ACM Press: Tampa, FL, 2006.
(36) Okruss, M.; Müller, R.; Hese, A. High-Resolution Ultraviolet Laser Spectroscopy on Jet-Cooled Benzene Molecules: Ground and Excited Electronic State Polarizabilities Determined from Static Stark Effect Measurements. *J. Chem. Phys.* **1999**, *21* (1), 10393−10402.
(37) McCall, D. W.; Douglass, D. C.; Falcone, D. R. Molecular Motion in ortho-Terphenyl. *J. Chem. Phys.* **1969**, *50* (9), 3839−3843.
(38) Dries, Th.; Fujara, F.; Kiebel, M.; Rössler, E.; Sillescu, H. H-NMR Study of the Glass Transition in Supercooled ortho-Terphenyl. *J. Chem. Phys.* **1988**, *88* (4), 2139−2147.
(39) Cummins, H. Z.; Hwang, Y. H.; Li, G.; Du, W. M.; Losert, W.; Shen, G. Q. Relaxation Dynamics in ortho-Terphenyl: Comparing β_K from Extended Mode Coupling Theory and Phenomenological Analyses. *J. Non-Cryst. Solids.* **1998**, *235*−*237*, 254−267.
(40) Naoki, M.; Endou, H.; Matsumoto, K. Pressure Effects on Dielectric Relaxation of Supercooled ortho-Terphenyl. *J. Phys. Chem.* **1987**, *91* (15), 4169−4174.
(41) Naoki, M.; Koeda, S. Pressure-Volume-Temperature Relations of Liquid, Crystal, and Glass of o-Terphenyl: Excess Amorphous Entropies, and Factors Determining Molecular Mobility. *J. Phys. Chem.* **1989**, *93* (2), 948−955.

(42) Torre, R.; Taschin, A.; Sampoli, M. Acoustic and Relaxation Processes in Supercooled Orthoterphenyl by Optical-Heterodyne Transient Grating Experiment. *Phys. Rev. E* **2001**, *64*, 061504.
(43) Leone, L. M.; Kaufman, L. J. Single Molecule Probe Reports of Dynamic Heterogeneity in Supercooled ortho-Terphenyl. *J. Chem. Phys.* **2013**, *138* (12), 12A524.
(44) Berne, B. J.; Pecora, R. *Dynamic Light Scattering: With Applications to Chemistry, Biology, and Physics*; John Wiley & Sons: New York, 1976.
(45) Lindsey, C. P.; Patterson, G. D. Detailed Comparison of the Williams−Watts and Cole−Davidson Functions. *J. Chem. Phys.* **1980**, *73* (7), 3348−3357.
(46) Petzold, N.; Schmidtke, B.; Kahlau, R.; Bock, D.; Meier, R.; Micko, B.; Kruk, D.; Rössler, E. A. Evolution of the Dynamic Susceptibility in Molecular Glassformers: Results from Light Scattering, Dielectric Spectroscopy, and NMR. *J. Chem. Phys.* **2013**, *138*, 12A510.
(47) Lombardo, T. G.; Debenedetti, P. G.; Stillinger, F. H. Computational Probes of Molecular Motion in the Lewis-Wahnström Model. *J. Chem. Phys.* **2006**, *125* (17), 174507−174516.
(48) Chong, S.-H.; Kob, W. Coupling and Decoupling between Translational and Rotational Dynamics in a Supercooled Molecular Liquid. *Phys. Rev. Lett.* **2009**, *102*, 025702.
(49) Chang, S. S.; Bestul, A. B. Heat Capacity and Thermodynamic Properties of o-Terphenyl Crystal, Glass, and Liquid. *J. Chem. Phys.* **1972**, *56* (1), 503−516.
(50) Aikawa, S.; Maruyama, Y.; Ohashi, Y.; Sasada, Y. 1,2-Diphenylbenzene (o-Terphenyl). *Acta Crytstallogr.* **1978**, *B34*, 2901−2904.
(51) Brown, G. M.; Levy, H. A. o-Terphenyl by Neutron Diffraction. *Acta Crystallogr.* **1979**, *B35*, 785−788.
(52) Bartsch, E.; Bertagnolli, H.; Chieuxp, P.; David, A.; Sillescu, H. Temperature Dependence of the Static Structure Factor of ortho-Terphenyl in the Supercooled Liquid Regime close to the Glass Transition. *Chem. Phys.* **1993**, *169* (3), 373−378.
(53) Tölle, A.; Schober, H.; Wuttke, J.; Fujara, F. Coherent Dynamic Structure Factor of ortho-Terphenyl around the Mode Coupling Crossover Temperature T_c. *Phys. Rev. E* **1997**, *56* (1), 809−815.
(54) Plazek, D. J.; Bero, C. A.; Chay, I.-C. Relaxations in Complex Systems. Section 1. Glass Transition and Related Topics. The Recoverable Compliance of Amorphous Materials. *J. Non-Cryst. Solids* **1994**, *172*−*174*, 181−190.
(55) Opdycke, J.; Dawson, J. P.; Clark, R. K.; Dutton, M.; Ewing, J. J.; Schmidt, H. H. Statistical Thermodynamics of the Polyphenyls. I. Molar Volumes and Compressibilities of Biphenyl and m-, o-, and p-Terphenyl Solid and Liquid. *J. Phys. Chem.* **1964**, *68* (9), 2385−2392.